Computational MR Image Analysis for Spinal Cord Injury Studies

K. Ming[1,2], R. Abugharbieh[1], C. F. Jones[2,3], A. Yung[4], P. Kozlowski[4], W. Tetzlaff[3], and P. A. Cripton[2,3]

[1]Department of Electrical and Computer Engineering, University of British Columbia, Vancouver, British Columbia, Canada, [2]Departments of Mechanical Engineering and Orthopaedics, University of British Columbia, Vancouver, British Columbia, Canada, [3]International Collaboration on Repair Discoveries, University of British Columbia, Vancouver, British Columbia, Canada, [4]UBC MRI Research Centre, University of British Columbia, Vancouver, British Columbia, Canada

Introduction

Research in the area of spinal cord injury has traditionally been carried out through biomechanical testing where animal spinal cords are exposed and subjected to mechanical injury [1,2]. However, a major limitation of this is the need to surgically expose the cord, which changes the physiological environment as well as the mechanical boundary conditions of the spinal cord by direct alteration of the bony canal, dura, and the cerebrospinal fluid (CSF) layer. We propose an alternative approach based on magnetic resonance imaging (MRI) and computational image deformation analysis techniques for the non-invasive study and quantitative assessment of spinal cords *in vivo* without exposure. We demonstrate that the proposed approach constitutes a novel advancement as it allows for the potential derivation of the causes, mechanisms, and tolerance parameters of myelopathy-related sustained compression of the spinal cord, as well as the measures used in the study of neuroprotection and regeneration of spinal cord tissue. Since this is all accomplished *in vivo*, we ensure that the physiological and biomechanical properties of the spinal cord and its environment are retained.

Methods

In vivo MR scans of the rat spinal cord, captured before and after applying a deformation, were acquired on a Bruker Biospec 7T MRI scanner (Ettlingen, Germany) using a 120 mm i.d. gradient coil and 70 mm i.d. quadrature birdcage RF coil. The anesthetized rat was mounted in the supine position on a cylindrical half shell with a custom-made device underneath that can be inflated to change the posture of the lumbo-sacral spine *in situ*. A heavily T1-weighted 3D FLASH scan was acquired with slab direction parallel to the lumbar spine axis (TE/TR = 3/15 ms, 50x50x25mm field of view, 195x195x390 um resolution, NA=2, acquisition time approximately 24 minutes with respiratory triggering). An identical scan with the same orientation and position was acquired after inflating the custom-made device to generate cord deformation.

The spinal cord was first segmented, using a user-guided procedure, from the surrounding anatomy (e.g. vertebrae and epidural contents) to facilitate subsequent registration of the cord images. The spinal cord, composed entirely of soft tissue, is flexible and does not move as a rigid body, thus necessitating a non-rigid registration process. However, the cord can undergo rotation and/or translation, combined with deformation, in response to certain external loading modes. We thus initialized the registration process by rigidly registering image pairs for global cord alignment, using a mutual-information-based approach, prior to performing B-spline-based non-rigid registration [3] to account for local deformations.

Results

Figure 1 shows example slices from the image we acquired of the undeformed *in vivo* rat spinal cord and column. In order to validate our non-invasive image-based cord deformation analysis approach, we applied known synthetic warping schemes – Warp 1 ('bending') and Warp 2 ('contortion') – to the MR data of the spinal cord. Deformation fields, generated using the proposed algorithm, were then compared against the known synthetic deformations applied to assess accuracy. The qualitative and quantitative results of the validation are shown in Figures 2 and 3, respectively. As shown in Figure 3, error increases with increasing deformation, because it is increasingly more difficult for the algorithm to determine the direction and amount of deformation for each voxel. Also shown in Figure 3, at 100% maximum deflection, beyond which deformations rarely occur, the percentage median error is approximately 5%. Note that for the *in vivo* rat cord, the mean dorsal-ventral spinal cord width was measured from the MR data to be 1.61 mm (range 1.18 – 2.79 mm; standard deviation 0.29 mm), measured across 64 slices (cord length of 25.60 mm). Qualitative results derived from images of the physical deformation of the rat spinal cord, using the custom-made inflation device, are shown in Figure 4.

Discussions & Conclusions

We have developed a novel *in vivo* MRI-based method for non-invasive analysis of myelopathy-related sustained compression of the spinal cord. Compared to current research approaches, which require exposure of the spinal cord, our method examines the progression of deformation leading to cord myelopathy without requiring surgical exposure, thereby retaining the physiological and biomechanical conditions. Accuracy was established by measuring the difference between a known (synthetically applied) deformation field and the field derived from our technique. Qualitative results presented in Figures 2 and 4 show that the deformation field lines match up accurately between locations in the spinal cord before deformation and the corresponding locations after deformation. Quantitatively speaking, the error levels achieved were consistently below 6%, even for large degrees of deformation up to the dorsal-ventral width of the spinal cord (100% deflection).

References. [1] Hung TK et al, J. Biomech. 14(4) (1981) 269-276. [2] Kwon BK et al, Spine 27(14) (2002) 1504-1510. [3] Rueckert D et al, IEEE Trans. Med. Imag. 18(8) (1999) 712-721.

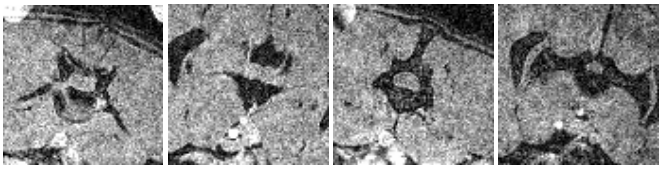

Figure 1: *Representative axial cross-sections from a rat spinal cord* in vivo.

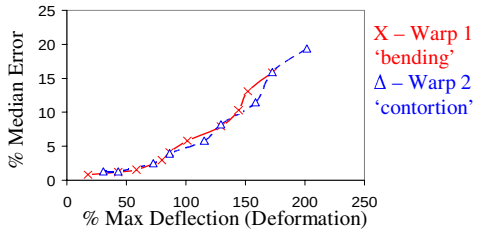

Figure 3: *Validation results showing accuracy of measured deformation, represented as median error between the known (synthetic) and automatically calculated (from MR images) deformation fields. Various levels of deformation of the original in vivo spinal cord data with Warp 1 ('bending') and Warp 2 ('contortion') are shown. Both the error and deformation extent are measured relative to the cord width.*

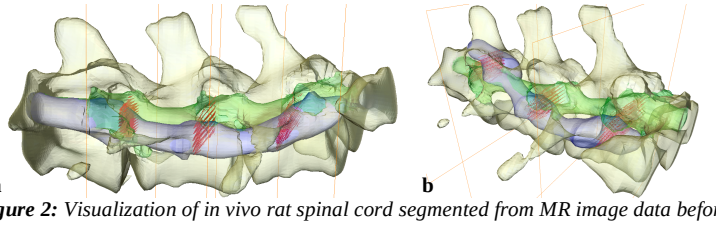

Figure 2: *Visualization of in vivo rat spinal cord segmented from MR image data before (green) and after (blue) applying a synthetic (a) Warp 1 ('bending'), and (b) Warp 2 ('contortion'). Corresponding deformation fields at 3 locations are overlaid (red lines). Vertebrae are only shown for the non-deformed position for clarity.*

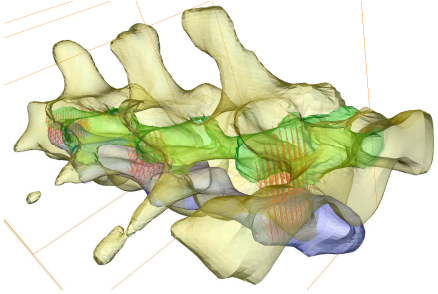

Figure 4. *Visualization of MR image of the in vivo rat spinal cord (including the vertebrae) before (green) and after (blue) a real deformation. Corresponding deformation fields at 3 locations are overlaid (red lines). Vertebrae are only shown for the non-deformed position for clarity.*